Biogeosciences Discuss., 9, 3381–3422, 2012
www.biogeosciences-discuss.net/9/3381/2012/
doi:10.5194/bgd-9-3381-2012

Biogeosciences
Discussions

New insights on the role of organic speciation in the biogeochemical cycle of dissolved cobalt in the southeastern Atlantic and the Southern Ocean

J. Bown, M. Boye, and D. M. Nelson

Institut Universitaire Européen de la Mer (IUEM), UMS3113, LEMAR, Technopôle Brest Iroise,
Place Nicolas Copernic, 29280 Plouzané, France

Received: 11 February 2012 – Accepted: 15 February 2012 – Published: 16 March 2012

Correspondence to: J. Bown (johann.bown@univ-brest.fr)

Published by Copernicus Publications on behalf of the European Geosciences Union.

Abstract

The organic speciation of dissolved cobalt was investigated in the subtropical region of the southeastern Atlantic, and in the Antarctic Circumpolar Current (ACC) and the northern Weddell Gyre in the Southern Ocean between 33°58′ S and 57°33′ S along the Greenwich Meridian during the austral summer of 2008. The organic speciation of cobalt was determined by Competing Ligand Exchange Adsorptive Cathodic Stripping Voltammetry (CLE-AdCSV) using nioxime as a competing ligand. The conditional stability constants ($\log K'_{\mathrm{CoL}}$) of the organic complexes of Co ranged between 17.9 and 20.1, and the concentrations of the organic ligands (L) between 26 and 73 pM. Most dissolved cobalt (DCo) was organically complexed in the water-column (60 to ≥99.9 %). There were clear vertical and meridional patterns in the distribution of L and the organic speciation of DCo along the section. These patterns suggested a biological source of the organic ligands in the surface waters of the subtropical domain and northern subantarctic region, potentially driven by the cyanobacteria, and a removal of the organic Co by direct or indirect biological uptake. The highest L:DCo ratio (e.g. $5.81 \pm 1.07\,\mathrm{pM\,pM^{-1}}$) observed in these surface waters reflected the combined effects of ligand production and consumption of DCo. As a result of these combined effects, the calculated concentrations of free, unbound Co ($[\mathrm{Co}']$) in subtropical and subantarctic surface waters were very low, generally between 10^{-19} and 10^{-17} M. In intermediate and deep waters, the South African margins can be a source of organic ligands, as it was suggested to be for DCo (Bown et al., 2011), although a significant portion of DCo (up to 15 %) can be stabilized and transported as inorganic species in those DCo-enriched water-masses. Contrastingly, the distribution of L did not suggest an intense biological production of L around the Antarctic Polar Front where a diatom bloom had recently occurred. Here $[\mathrm{Co}']$ can be several orders of magnitude higher than those reported in the subtropical domain, suggesting that cobalt limitation was unlikely in the ACC domain. The almost invariant L:DCo ratio of ∼1 recorded in these surface waters also reflected the conservative behaviours of both the organic ligands and DCo. In deeper waters relatively higher ligand concentrations were observed in waters previously identified as DCo sources (Bown et al., 2011). At those depths the eastward increase of DCo could be associated with a large scale transport and remineralisation of DCo as organic complexes; here, the fraction stabilized as inorganic Co was much lower but still significant (up to 25 %) in the low oxygenated Upper Circumpolar Deep Waters. The organic speciation may thus be a central factor in the biogeochemical cycle of DCo in those areas, playing a major role in the bioavailability and the geochemistry of Co.

1 Introduction

The organic complexation of Co likely plays a significant role in the biogeochemical cycle of dissolved cobalt (DCo) in the ocean, affecting both its bioavailability (Ellwood and van den Berg, 2001; Ellwood et al., 2005; Saito and Moffett, 2001; Saito et al., 2004) and its solubility in oxygenated seawater (Moffett and Ho, 1996). Electrochemical methods have been used to study the potential affinity of cobalt with dissolved organic matter, that also allow the determination of the total concentration of organic Co-binding ligands and conditional stability constants of the organic complexes. Such measurements can lead to improved understanding of the biogeochemical cycle of Co in the open ocean. However studies of the organic speciation of DCo in the ocean are still scarce (Ellwood et al., 2005; Saito and Moffett, 2001; Saito et al., 2005; Yang and Van den Berg, 2009). The distribution of Co-binding organic ligands exhibits increasing concentration with depth (Ellwood et al., 2005), and relative maxima (or minima) in the euphotic layer (Ellwood and van den Berg, 2001; Saito and Moffett, 2001), with a rather uniform distribution or increasing concentrations in deeper waters (Ellwood and van den Berg, 2001). This probably reflects the spatial variety of the ligand sources and sinks in different ocean waters as well as the seasonal variability of these terms. As far as we know, no data have previously been reported for Co-binding ligand concentrations in deep waters below 2000 m.

The few studies on the organic speciation of cobalt have shown that DCo occurs predominantly as strong organic complexes in the euphotic layer of subtropical ocean regions (Noble et al., 2008; Saito and Moffett, 2001; Saito et al., 2004, 2005). The sources of these ligands are not well characterized, but the release of Co-binding ligands by cyanobacteria has been suggested from laboratory and field studies (Saito and Moffett, 2001; Saito et al., 2002, 2005). Conversely, elevated ligand concentrations have been reported at the depth of the chlorophyll-*a* maximum in the Southern Ocean, south of the Polar Front where cyanobacteria were absent (Ellwood et al., 2005). This suggests that other photosynthetic organisms, as well as other ligand sources such as the release of organic compounds during phytoplankton cell degradation, should be also considered. The chemical nature of the ligands is also not known, but it has been suggested that vitamin B_{12} (cobalamine) and its degradation products could strongly bind Co (Saito et al., 2010, 2002), since Co is the structural atom of this vitamin. Siderophores such as desferrioxamine B or siderophore-like compounds could also form extremely strong complexes with Co (Duckworth et al., 2009). Cobalt may also be bound with humic substances in seawater (Yang and Van den Berg, 2009) although these complexes may be weaker than those formed with the vitamin B_{12}, the coenzyme B_{12} (Ellwood and van den Berg, 2001) and desferrioxamine B (Duckworth et al., 2009).

Here we report the distribution of Co-binding organic ligands in the water-column of the subtropical domain in the southeastern Atlantic and of the Antarctic Circumpolar Current and the Weddell Gyre in the Southern Ocean along the 0° meridian to investigate their biogeochemical cycle in contrasted areas and different water-masses. We use this information, along with the distribution of DCo recently described in the same area (Bown et al., 2011) to investigate the impact of the organic speciation on the biogeochemical cycle of DCo in this region.

2 Methods

2.1 Sampling

Samples were collected during the multidisciplinary MD166 BONUS-GoodHope cruise that took place in the austral summer 2008, during the International Polar Year (02/13/08–03/24/08) on board the French R/V *Marion-Dufresne II* sailing from Cape Town, South Africa, to 57° S along the Greenwich Meridian in the Southern Ocean (Fig. 1).

The samples for the determination of DCo and its organic speciation were collected from the upper 2100 m at 7 stations and from the entire water column (0–4000 m) at 5 stations, with 10 acid-cleaned 12 L GO-FLO bottles (General Oceanics) modified with PTFE rings, attached to a Kevlar wire and closed using Teflon-coated messengers. The samples were collected in acid-cleaned LDPE Nalgene bottles after online filtration with a 0.22 µm Sartobran 300 (Sartorius) cartridge under pure N_2 pressure (99.99 % N_2, 1 bar) in a pressurized clean container (class 100). Samples collected to assess the organic speciation of Co were immediately frozen at −20 °C, and those collected for DCo analyses were acidified at pH∼2 using ultrapur hydrochloric acid (ultrapurHCl, Merck) and stored in double bags at dark and ambient temperature. The determination of the organic speciation of Co and the analyses of DCo were conducted in a clean room in the shore-based laboratory, about 3 months and 18 months after the samples collection, respectively.

2.2 Analytical procedures

2.2.1 Dissolved cobalt

The concentrations of DCo were measured in acidified and UV-digested samples by Flow Injection Analysis and chemiluminescence detection as described in Bown et al. (2011). The reagent blank from acid/buffer additions and column rinse was

5.90 ± 1.24 pM (standard error, $n = 40$) in MilliQ, yielding a detection limit (3σ) of 3.72 pM ($n = 40$) (Bown et al., 2011).

2.2.2 Organic speciation of dissolved cobalt

The organic speciation of DCo was determined by complexing capacity titrations in the filtrate by Competing Ligand Exchange-Adsorptive Cathodic Stripping Voltammetry (CLE-AdCSV) with ligand competition against nioxime at pH~8.1 (Zhang et al.,1990; Ellwood and van den Berg, 2001).

Two identical voltammetric devices, consisting of a mercury-drop electrode (model VA 663, Metrohm, Switzerland) connected to a µAutolab potentiostat (Type II, Ecochemie) and an autosampler (Sample Processor 778, Metrohm), were used simultaneously to increase the sample throughput. The reference electrode was double junction, Ag/AgCl, 3 M KCl, with a salt bridge filled with 3 M KCl, and the counter electrode was a glassy carbon rod.

The seawater pH was buffered at 8.1 using borate buffer (H_3BO_3, Sigma Ultra). The borate stock solution (1 M boric acid/0.3 M NaOH, Merck) was cleaned by running through a Chelex-100 column and was used at a final concentration of 10 mM. A stock solution of 0.1 M nioxime (1,2-cyclohexanedione dioxime, Sigma Aldrich) was prepared in 0.2 M sodium hydroxide (Merck). A final nioxime concentration of 0.1 mM was used for the titrations. Samples were titrated with Co using a stock Co-solution of 10^{-8} M (Spectrosol solution, Sigma Aldrich) prepared in 0.05 % ultrapur hydrochloric acid, which was added in 10 increments on the order of 10 pM to 200 pM Co ranging between 0 and 250 pM. Any remaining sample was pipetted into a 12th vial, and used for the first measurement to condition the voltammetric cell. The 30 mL Teflon vials containing the sample and the reagents (Co standard, borate buffer and nioxime solution) were left for equilibration for 12–15 h, at room temperature in a laminar flow hood.

The twelve equilibrated solutions were sequentially (starting from the lowest cobalt addition) and automatically transferred to the voltammetric Teflon cell. After the cell has been automatically emptied, 3 mL of each solution were first pumped to rinse the system followed by 15 mL that were used for the analysis. The voltammetric cell was not rinsed during the titration, but it was rinsed at its end with acidified MilliQ (HCl ultrapur, $1\,^{0}/_{00}$) and MilliQ water.

After purging each solution with O_2-free nitrogen (99.999 %) for 3.25 min, the measurements were made using a deposition time onto the mercury drop of 180 s at an adsorption potential of −0.7 V, followed by a 10 s equilibration period and a negative potential scan from −0.7 to −1.2 V using the differential pulse waveform with a pulse amplitude of 100 mV, a modulation time of 10 ms, an interval time of 100 ms and a step potential of 1.5 mV. Repeated (3 times) scan rates were made for each measurement, and the mean peak height of the reduction current of the Co-nioxime complex was used to resolve the titration.

The conditional stability constant for the Co-ligand complexes (CoL) was defined as:

$$K'_{\mathrm{CoL}} = [\mathrm{CoL}]/([\mathrm{Co}^{2+}][\mathrm{L}']) \quad (1)$$

where [CoL] is the organic Co complexes concentration, $[\mathrm{Co}^{2+}]$ is the free Co ion concentration and [L′] is the concentration of organic ligands not bound to Co and were calculated by linear least-squares regression of the data fitted to the Ruzic/van den Berg following equation (Ruzic, 1982; van den Berg, 1982; van den Berg and Kramer, 1979), from the slope and the Y-intercept respectively:

$$[\mathrm{Co}_{\mathrm{labile}}]/[\mathrm{CoL}] = [\mathrm{Co}_{\mathrm{labile}}]/[\mathrm{L}] + (\alpha_{\mathrm{Co}'} + \alpha_{\mathrm{CoNioxime2}})/([\mathrm{L}]K'_{\mathrm{CoL}}) \quad (2)$$

The inorganic side reaction coefficient for Co was taken as $\log \alpha_{\mathrm{Co}'} = 1.74$ (Turner et al., 1981), and for the $\mathrm{CoNioxime}_2$ complexes as $\log \alpha_{\mathrm{CoNioxime2}} = 7.62$ (using $\log\beta'_{\mathrm{CoNioxime2}} = 15.62$ at salinity of 35; Zhang et al., 1990, and $[\mathrm{Nioxime}_2] = 0.1$ mM), providing an analytical detection window (Zhang et al., 1990) of $10^{6.62}$ to $10^{8.62}$ for the detection of α_{CoL} (equal to [L′] x K'_{CoL}).

The concentration of labile Co $[Co_{labile}]$ in each aliquot was calculated from the triplicate measured peak height as:

$$[Co_{labile}] = i_p/S \tag{3}$$

where S is the sensitivity calculated from the linear part of the titration and i_p the peak height obtained at the reduction potential of the Co-Nioxime$_2$ complex.

The concentration of CoL that equilibrates with the added nioxime and Co was calculated in Eq. (2) from:

$$[CoL] = [DCo] - [Co_{labile}] \tag{4}$$

where [DCo] is the dissolved Co concentration including the Co additions.

Then [L], K'_{CoL} and their standard deviations (stdv) are calculated from the slope and the Y-axis intercept of the linear least-squares regression of $[Co_{labile}]/[CoL]$ as a function of $[Co_{labile}]$ (Eq. (2)) fitted for a single ligand. The reproducibility obtained from triplicate analysis of a filtered seawater sampled at 30 m depth of S5 station was better than 10 % for the ligand concentration determinations (e.g. 38.9 ± 3.47 pM, $n = 3$), and better than 1 % for the conditional stability constant (e.g. log value of 18.1 ± 0.21, $n = 3$).

The free metal ion concentration $[Co^{2+}]$ originally present in the seawater is calculated with the following quadratic equation:

$$[Co^{2+}]^2 \alpha_{Co'} K'_{CoL} + [Co^{2+}](\alpha_{Co'} + K'_{CoL}[L] - K'_{CoL}[DCo]) - [DCo] = 0 \tag{5}$$

Then the inorganic Co concentration ([Co′]) originally present in the seawater is calculated from:

$$[Co'] = \alpha_{Co'}[Co^{2+}] \tag{6}$$

The concentration of the organic cobalt ([CoL]) in the seawater is obtained by difference from the DCo concentration and the inorganic metal concentrations as:

$$[CoL] = [DCo] - [Co'] \tag{7}$$

The fraction (%) of Co occurring as organic species is calculated as $([CoL]/[DCo])^{*}100$.

3 Results

3.1 Hydrography

The cruise track crossed the subtropical domain southwest of South Africa (stations L1, S1, L2), the frontal systems (Belkin and Gordon, 1996; Orsi et al., 1995) of the Antarctic Circumpolar Current (ACC; stations S2 to L7) and entered the Weddell Gyre (station S5), as shown in Fig. 1. The water-masses and circulation patterns of the study area are given in detail in Bown et al. (2011). Salinity, potential temperature and dissolved oxygen vertical sections are given Fig. 2 (Speich et al., 2012) and a glossary is provided here to report the main water-masses, their origin and associated characteristics, and depth ranges (Table 2).

3.2 Biogeochemical features of the studied area

Biogeochemical features are described and detailed elsewhere (Le Moigne et al., 2012). Several biogeochemical provinces were crossed along the section, generally characterized by a southward increase of macronutrient concentrations much of which occurred near the frontal boundaries. Briefly, the subtropical domain (L1 to S2 stations) dispatched low nitrate, phosphate and silicate concentrations, and a subsurface Chl-*a* maximum with concentrations ranging between 0.3 and 0.6 $\mu g\,L^{-1}$ (Fig. 3), featuring oligotrophic conditions (Le Moigne et al., 2012). In the Polar Frontal Zone, on the northern side of the PF, nitrate and phosphate concentrations increased and ammonium exhibited a subsurface maximum of ∼1.25 µM (Le Moigne et al., 2012). Chl-*a* concentrations ranged between 0.2 and 0.4 $\mu g\,L^{-1}$, while phaeopigments (e.g. degradation products of Chl-*a*) displayed their highest values recorded along the section (Le Moigne et al., 2012). All these features indicated that a vast bloom of diatom occurred before the start of our observations in the vicinity of the PF (Le Moigne et al., 2012). Macronutrients concentrations increased in the high-nutrient, low-chlorophyll area ((Minas et al., 1986) between stations S4 and L7) while Chl-*a* concentrations were low

(<0.3 µg L^{-1}; Fig. 3). A slight increase of Chl-*a* concentration up to 0.3 µg L^{-1}(Fig. 3), associated with an increase of phaeopigments and a slight decrease of silicate concentrations, was recorded at the southern end of the section at station S5, located in the Weddell Gyre, possibly indicating a recent small bloom of diatoms (Le Moigne et al., 2012).

3.3 Dissolved cobalt

DCo concentrations ranged between 5.73 ± 1.15 pM and 72.9 ± 4.51 pM (standard deviations, based on triplicate analyses) along the section (Table 1; Bown et al., 2011). The distribution of DCo was nutrient-like in surface waters of the subtropical domain, with the lowest concentrations measured in the highest Chl-*a* maxima (Fig. 3; Bown et al., 2011). In deeper waters DCo distributions showed increasing concentrations below the nutricline, and relative higher concentrations in the intermediate (e.g. I-AAIW) and deep (e.g. SE-NADW) water-masses that have been in contact with the continental margins of South Africa (Bown et al., 2011). In contrast, the vertical distribution of DCo showed scavenged-type behavior in the ACC domain and conservative distribution in the Weddell Gyre (Fig. 3; Bown et al., 2011). At depth, the highest DCo concentrations were observed in the cores of the low-oxygenated Upper Circumpolar Deep Waters (e.g. A-UCDW and DP-UCDW; Bown et al., 2011), and relatively high values were also observed in the core of A-AAIW; these waters originated from the southwest Atlantic and the Drake Passage. In the bottom waters, lower DCo concentrations were observed in the recently formed AABW near the Weddell Gyre seafloor as compared to the higher values observed in the older variety of AABW that flowed north of the Agulhas Ridge (Fig. 3).

3.4 Organic Co-binding ligands

The plots of $[\mathrm{Co}_{\mathrm{labile}}]/[\mathrm{CoL}]$ versus $[\mathrm{Co}_{\mathrm{labile}}]$ (e.g. Eq. 2) were linear, indicating that the van den Berg/Ruzic equation fitted to 1:1 ligand:Co could be used to describe linearised data (Ruzic, 1982; van den Berg, 1982). The organic Co-binding ligand concentrations ([L]) ranged between 26.3 ± 1.9 pM at the SACCF (at 1117 m depth at station S4) and 71.9 ± 2.8 pM (standard deviation of triplicate analyses) in the subtropical domain (STZ) (at 15 m depth at station L2), as reported in Table 1, with a mean L value of 45.5 ± 9.4 pM ($n = 142$) (± corresponds to the standard deviation from the mean concentration unless otherwise stated). The distribution of Co-binding ligands displayed relative [L] maxima in the Chl-*a* rich layer of the subtropical domain and northern subantarctic region (∼50 pM at stations L1, S1 and S2; ∼70 pM at station L2; Fig. 3), as well as relative decreases (to 30 and 40 pM) at the depth of the DCo minimum (Fig. 3). High ligand concentrations (up to 72 pM) and the highest excess of ligands (mean value of 41.1 ± 15.1 pM, $n = 7$) over DCo (mean value of 12.8 ± 5.68 pM, $n = 7$) concentrations were observed in the upper 150 m at stations L2 and S2, both marked by a subsurface maximum in Chl-*a*concentrations, with the highest Chl-*a* values recorded along the section concomitant with the lowest recorded DCo (Fig. 3). The highest [L]/[DCo] ratio was also found in the surface waters at L2 and S2 stations with a mean of 3.90 ± 2.10 pM pM^{-1} (Figs. 4–5), while the overall mean [L]/[DCo] ratio was 1.22 ± 0.78 pM pM^{-1} ($n = 142$). Below the nutricline [L] increased to values similar or slightly higher than those in surface waters (Fig. 3). In intermediate and deep waters, L distributions closely followed those of DCo and were in similar concentration ranges (Table 1, Fig. 3). Relatively high ligand concentrations were found in the cores of I-AAIW and A-AAIW (e.g. 49.4 ± 2.4 pM, $n = 6$; and 50.8 ± 11.1 pM, $n = 5$, respectively), as well as in the cores of SE-NADW and AABW (respective mean value of 51.0 ± 3.9 pM, $n = 7$, and 44.9 ± 1.9, $n = 3$). Southward of the central ACC the vertical distribution of L was fairly conservative in the upper 150 m with a mean [L] of 44.0 ± 8.7 pM ($n = 22$) (Fig. 3, Table 1). In these surface waters ligand concentrations (mean value 42.8 ± 7.89 pM, $n = 21$) did not significantly exceed DCo levels (mean value 42.5 ± 7.23 pM, $n = 21$), that is also reflected by a fairly invariant [L]/[DCo] ratio of ∼1 pM pM^{-1} (Figs. 4–5). In intermediate and deep waters the concentrations and distributions of L were similar to those of DCo (Fig. 3), with relatively high values of [L] recorded in the core of A-AAIW (54.5 ± 9.16 pM, $n = 6$), in A-UCDW (46.7 ± 9.02 pM, $n = 4$) and in DP-UCDW (46.5 ± 9.15 pM, $n = 10$). [L] decreased southward in the AABW from 39.2 ± 1.74 pM ($n = 2$) at S3 to 32.7 ± 0.78 pM ($n = 2$) at the southernmost station S5.

The overall mean conditional stability constant ($\log K'_{CoL}$) was 18.8 ± 0.38 ($n = 142$), and was not significantly different in the upper 150 m (18.7 ± 0.46, $n = 41$) and intermediate and deep waters (18.9 ± 0.33, $n = 101$). The standard deviation of the conditional stability constants varied between (log values) 0.05 and 0.6, the highest values being reported in the samples where the initial DCo concentration was close or greater than the ligand concentration (Table 1). This bias is due to the absence of curvature of the titration which causes the intercept with the Y-axis (Eq. 2) to be small and the error to be relatively large.

3.5 Organic speciation of dissolved cobalt

The organic complexation overall dominated the chemical speciation of DCo along the section, with DCo being organically bound at ~60 to ≥99.9 %. In the surface waters of the subtropical and northern subantarctic domains, DCo was consistently >99.9 % organically bound (Table 1). Hence inorganic Co concentrations ([Co′]) were extremely low in these surface waters (3×10^{-20}–10^{-17} M), whereas organic Co concentrations ([CoL]) were almost exactly equal to [DCo], ranging between ~5 and ~15 pM (Table 1). At intermediate depths, in the cores of I-AAIW and A-AAIW, [Co′] was generally higher than in the surface layer with concentrations ranging from ~1.0×10^{-18} to 9.0×10^{-12} M and the organic Co represented ~60 to >99.9 % of DCo, lower than in the surface layer (Table 1). The deep SE-NADW was also characterized by higher inorganic Co levels (4×10^{-18}–7×10^{-12} M), with organic Co representing a relatively lower fraction of DCo (88 to >99.9 %) compared to surface waters (Table 1). In the AABW, [Co′] varied between 6×10^{-19} and 3×10^{-12} M and organic Co represented ~93 to >99.9 % of DCo. Southward of the central ACC the organic complexation still dominated the speciation of DCo, but its magnitude in surface waters was generally lower (~60 to >99.9 %) than in the northern part of the section (Table 1). The higher DCo concentrations in the more southerly surface waters compared to the north of the section (Fig. 3), combined with the overall higher proportion of inorganic Co, led to higher inorganic Co concentrations, which could be as high as 11 pM (Table 1). As a result of higher [DCo], the organic Co concentrations were also higher in those surface waters (e.g. 20–55 pM) compared to values recorded in the surface waters of the northern part of the section (e.g. 5–15 pM). In deeper waters the two varieties of UCDW were characterized by the organic Co representing ~75 to ≥99.9 % of DCo, and by [Co′] ranging between $\sim 9 \times 10^{-19}$ and $\sim 8 \times 10^{-12}$ M, in the same range than those reported in surface waters of this area (Table 1). In the AABW, [Co′] varied between $5–10 \times 10^{-19}$ M (at station S3) and 3×10^{-12} M (at station S5) and the organic Co represented 90 % (at station S5) to more than 99 % (at station S3) of DCo (Table 1).

4 Discussion

4.1 Cobalt speciation determinations

In most cases, the CSV peak height was found to increase linearly with Co additions, indicating that relatively strong Co-binding organic ligands were already saturated with Co, and/or that the nioxime was out competing the natural ligands for Co (Fig. 6a). The titration curves were however always below the theoretical curve that would be obtained if no ligand was present in the sample or if the ligands were outcompeted for binding Co by the addition of nioxime. Hence there was in any case a larger fraction of detectable non-labile Co (e.g. bound to strong ligands) with the labile fraction (e.g. bound to nioxime) remaining far below the DCo concentration (Fig. 6a). These observations suggest that strong organic ligands saturated with Co were initially present in the samples, and that the organic complexes were not easily exchangeable for Co. The saturation of the organic Co-binding ligands with Co has been previously reported in oceanic waters (Saito and Moffett, 2001; Zhang et al., 1990). As stated above, the conditional stability constant of the ligand (K'_{CoL}) could not be calculated accurately in these conditions. Some titrations showed a curvature at low Co additions, indicative of the presence of free Co-binding sites (Fig. 6b). In the other cases the Co organic speciation was dominated by complexation with strong organic ligands that occurred at concentrations in the same range as those of [DCo], with no evidence for any large excess of free Co-binding sites that are titrated by additional Co (Fig. 4). To account for the absence of curvature in the titrations it is possible that the analytical detection window used in our study (e.g. centred on $\alpha_{CoNioxime2} = 10^{7.62}$) was rather low to competitively equilibrate with the strong ligands naturally present in the samples ($\alpha_{CoL} = 10^{8.56\pm0.47}$, $n = 142$). For instance, if Co(III)-L complexes were present, such as those that could be formed with vitamin B_{12} (Menzel and Spaeth, 1962) or desferrioxamine B (Duckworth et al., 2009) it is conceivable that they were outcompeting any other organic ligands such as nioxime to bind Co since Co(III) chelates have much higher thermodynamic stability constants than their corresponding Co(II) complexes (Saito and Moffett, 2001). Reported conditional stability constants with the synthetic ligand EDTA indeed suggest that in addition to Co(II) inorganic species being presumably more abundant (and soluble) than Co(III) inorganic species in the ocean waters (Cosovic et al., 1982; Moffett and Ho, 1996), the organic complexes formed with Co(III) are stronger (e.g. $\log K_{Co(III)EDTA} = 41.4$; Xue and Traina, 1996) than those formed with Co(II)(e.g. $\log K_{Co(II)EDTA} = 16.45$; Martell and Smith, 1977). On the other hand it is also possible that any ligands in excess of Co were masked by the complexation with another metal ion, especially with nickel, which may be present at a much greater abundance than Co and has shown similar binding strength of organic complexes (Saito and Moffett, 2001).

4.2 Distribution and cycle of the organic Co-binding ligands

4.2.1 Comparison with other studies

Relatively few studies of Co-binding ligand distributions have been reported in the open ocean, but they provide ranges of ligand concentrations of the same general magnitude reported here (Fig. 7). The distributions of [L] recorded in the Sargasso Sea at the BATS (Bermuda Atlantic Time-series Study) station show an overall excess of L over DCo in the euphotic layer associated with relative maxima of [L] in the chlorophyll maximum, while the difference between L and DCo decreased in deeper waters (Saito and Moffett, 2001), similar to the trends observed in this study in the subtropical domain and the subantarctic region (Fig. 7). In the Atlantic sector of the Southern Ocean, [L] exceed [DCo] in surface waters south of the Polar Front whereas the reverse was found to the north (Ellwood et al., 2005). Contrastingly, the difference between [L] and [DCo] remained almost constant across the Polar Front in this study and rather small in the surface waters southward of the central ACC (Fig. 5). An overall excess of DCo over L was also observed in the surface waters of the North Atlantic (Ellwood and van den Berg, 2001; Fig. 7). In deep waters below 150 m, there was no statistically significant correlation between [L] and [DCo] ($r^2 = 0.316$, $n = 119$) when all data available worldwide were considered. However L concentrations were overall higher than or in the same range as DCo in the study reported here, similar to other deep ocean waters except at some depths in the deep North Atlantic (Ellwood and van den Berg, 2001) and North of the Polar Front (Ellwood et al., 2005).

The comparison of the conditional stability constants suggests 1 to 5 orders of magnitude higher values in this study ($10^{17.9}$ to $10^{20.3}$) than those previously reported in oceanic waters (e.g. $10^{15.6}$ to $10^{17.2}$; (Ellwood and van den Berg, 2001; Ellwood et al., 2005; Saito and Moffett, 2001). The discrepancy can reflect differences in the chemical nature of the organic ligands, but it can also be due to differences in the analytical methods used, particularly with the choice of the competing synthetic ligand (nioxime versus dimethylglyoxime) and the detection window. For instance, Ellwood and van den Berg (2001) used a much lower detection window (centered on $\alpha_{\mathrm{CoNioxime2}} = 4.7$) and a higher pH (9.1) than we did (7.6 and 8.1, respectively), allowing the detection of weaker Co organic complexes than in the present study. Comparability between studies is even more difficult since there is not yet an intercomparison standard for ligand concentration and stability constant determinations. Given that vitamin B_{12} appears to be a frequently discussed complexing ligand for DCo, perhaps a chelexed and UV-digested, vitamin B_{12}-amended seawater sample of a predetermined concentration may be a useful option for the use of a standard to consider in future studies.

4.2.2 Cycle of the organic ligands along the section

The sources and the cycle of the organic Co-binding ligands in the ocean are not well known (Saito et al., 2001, 2005, 2010). In the present study the relative [L] maxima observed within or close to the Chl-*a* rich layers in the subtropical domain and the northern subantarctic zone (stations L1, S1, L2, S2; Fig. 3) suggested biological production of Co-binding ligands in those waters. Additionally the relative decreases of [L] observed in these Chl-*a* rich layers, but at different depths concomitant with relative minima of DCo (L1, S1 and S2 stations; Fig. 3), suggest biological uptake of L, probably as CoL complexes, and/or their biological degradation. The highest [L]/[DCo] ratio recorded in the section was found in the surface waters marked by the highest subsurface maximum in Chl-*a* concentrations, where high [L] (up to 72 pM) and the strongest depletion of DCo were also observed (at L2 and S2; Figs. 3–4). Hence the highest [L]/[DCo] ratio probably reflected biological production of ligands and uptake of DCo in those surface waters. A linear relationship between the integrated concentrations of Chl-*a* and [L] was obtained in the top 100 m of the subtropical and the northern subantarctic domains, which became stronger when stations L1 to S2 were considered: $[\text{Chl-}a]_{\text{int. } 0--100\text{m}} = 0.004^{*}[\text{L}]_{\text{int. } 0--100\text{m}} + 11.9$ ($r^2 = 0.781$, $n = 4$), further suggesting that phytoplankton could be a significant source of organic Co-binding ligands in those waters. For instance the cyanobacteria *Synechococcus sp.* and *Prochlorococcus sp.*, which often dominate the picophytoplankton assemblage in oligotrophic regions

Title Page
Abstract | Introduction
Conclusions | References
Tables | Figures
◀| |▶
◀ ▶
Back | Close
Full Screen / Esc
Printer-friendly Version
Interactive Discussion

(Partensky et al., 1999; Zhang et al., 2008a), are able to produce organic Co-binding ligands under different Co (and zinc) growth conditions as inferred by incubation experiments (Saito et al., 2002, 2005). It has also been suggested that biological production by *Prochlorococcus* and *Synechococcus sp.* can be the main source of L in the surface waters of the Sargasso Sea (Saito and Moffett, 2001). Similarly, production by cyanobacteria may be sufficient to cause the observed relative maxima of [L] in the surface waters of the subtropical waters in the present study.

The chemical nature of L is virtually unknown. However cyanobacteria have shown to be able to synthetize vitamin B_{12} (Bonnet et al., 2010) in which Co occurs as the central atom. Conditional stability constants of Co complexes with vitamin B_{12} ($\log K'_{\mathrm{Co-B12}}$) and coenzyme B_{12} ($\log K'_{\mathrm{Co-coB12}}$) of 16.4 and 15.5, respectively, have been reported using a detection window centred on $\alpha_{\mathrm{CoNioxime2}}$ of 4.7 (Ellwood and van den Berg, 2001). The mean conditional stability constant reported in the present study in the 0–150 m surface layer ($\log K'_{\mathrm{CoL}} = 18.8 \pm 0.59$, $n = 19$) at a much higher detection window (centred on $\alpha_{\mathrm{CoNioxime2}}$ of 7.6) is 2 to 3 orders of magnitude higher than those of vitamin B_{12} and coenzyme B_{12} Co-complexes. It is possible that vitamin B_{12} or compounds of similar nature have stronger affinity for Co than it has been reported previously, such that they would have been detected in the present study. Hence vitamin B_{12} or compounds of similar nature may have accounted for a significant portion of the organic ligands detected in the surface waters of the subtropical domain.

The conditional stability constants of Co-L complexes in this domain were in the same ranges in deep waters ($\log K'_{\mathrm{CoL}} = 18.9 \pm 0.42$, $n = 45$) as in surface waters ($\log K'_{\mathrm{CoL}} = 18.8 \pm 0.59$, $n = 19$), suggesting vertical export of L produced in surface waters and/or production in deep waters, with the L produced in deep waters having a chemical nature (or at least an affinity for Co) similar to those produced near surface. Furthermore the rather invariant [L]/[DCo] ratio's of ~1 pM pM^{-1} in intermediate and deep waters in this domain (Fig. 4) suggests that similar sources and sinks were impacting cycles of both the organic ligands and Co in the deep ocean. For instance, the deep distribution of DCo indicates remineralization and inputs from the margins of South

Africa with lateral advection of enriched intermediate (I-AAIW) and deep (SE-NADW) waters to the southeastern Atlantic Ocean (Bown et al., 2011). In these water-masses the distribution of L closely followed the DCo distribution and the concentrations were on the same range (Fig. 3; Table 1). Peculiarly, relatively high [L] was observed in the cores of I-AAIW (49.4 ± 2.4 pM, $n = 6$) and SE-NADW (51.0 ± 3.9 pM, $n = 7$). This suggests that the South African margins could also be a source of organic Co-binding ligands.

The surface distribution of L shifted southward within the ACC domain, where L concentrations paralleled those of DCo in surface waters with no evidence of high production of L (Fig. 3). There was no significant relationship between vertically integrated L and Chl-*a* concentrations in these surface waters, especially in the post-diatom-bloom area observed around the Antarctic Polar Front (Le Moigne et al., 2012), and no subsurface maxima of L. These observations argue against an intense biological source of L in this domain, either directly by L production by diatoms or other phytoplankton taxa, or indirectly due to cell lysis or bacterial degradation of the organic matter. These features contrast with the observations gathered south of the Polar Front at 20° E (Ellwood et al., 2005) which suggested an indirect production of L due to degradation of molecules released by phytoplankton, possibly after cell death (Ellwood et al., 2005); in that study Chl-*a* concentrations were twice as high as those reported here at the same latitude. In contrast, the distribution of L remained fairly constant within the euphotic layer in this study (stations S3 and L5; Fig. 3) indicating a balance between the production and the removal of L. The almost invariant [L]/[DCo] ratio of ~1 recorded in these surface waters (Figs. 4–5) and the uniform distributions of L and DCo in the surface layer also reflect conservative behaviour (or a balance between sources and sinks) of both L and DCo. Conditional stability constants of Co-L complexes in the surface waters of the ACC and the Weddell Gyre ($\log K'_{\mathrm{CoL}} = 18.6 \pm 0.32$, $n = 45$) were in the same range as those reported in the subtropical and northern subantarctic domains ($\log K'_{\mathrm{CoL}} = 18.8 \pm 0.59$, $n = 19$), which suggests that the ligands were of the same chemical nature in the surface waters of the whole section, whereas the nano- and picoplankton assemblages were dominated by different taxa (Beker et al., 2012), which might drive biological production of chemically different L. Below the nutricline [L] increased with depth at some stations (e.g. L6 and S4; Fig. 3), indicating possible remineralisation of L by bacterial activity there. In intermediate and deep waters the concentrations and distributions of L were similar to those of DCo (Fig. 3), which were also reflected by almost invariant [L]/[DCo] ratios of $\sim 1\,\mathrm{pM\,pM^{-1}}$ (Fig. 4). This suggests, as in the northern part of the section, that the deep cycles of L and DCo were impacted by similar sources and sinks, which have been described for DCo in Bown et al. (2011). DCo distributions and physical hydrodynamics suggest remineralisation and inputs from the Drake Passage and the southwestern Atlantic to the 0° meridian along the fast eastward flow of the Antarctic Circumpolar Current in the cores of A-AAIW and A-UCDW north of the Polar Front, as well as in the DP-UCDW south of the Polar Front (Bown et al., 2011). The concentration and distribution of L were similar to those of DCo in those intermediate and deep water-masses with relative high values (A-AAIW: 54.5 ± 9.16 pM, $n = 6$; A-UCDW: 46.7 ± 9.02 pM, $n = 4$; DP-UCDW: 46.5 ± 9.15 pM, $n = 10$; Fig. 3). This suggests that remineralisation and transport of ligands from lithogenic sources over long distance water-masses circulation could be a source of L in deep waters.

4.3 Possible implications for the bioavailability of cobalt

Cobalt may play an important physiological role in phytoplankton metabolism and growth, as it is involved in the activity of carbonic anhydrase and hydrolytic enzymes (Morel et al., 2003) and in the structure of the vitamin cobalamin (B_{12}). Culture experiments have shown that *Prochlorococcus sp.* have an absolute Co requirement for growth (Saito et al., 2002). Classically in growth experiments the addition of a synthetic ligand (EDTA, NTA or DTPA) controls the speciation of Co, and it is assumed that only the inorganic Co^{2+} species not bound to the added synthetic ligand are available for the biological uptake (Sunda and Hunstman, 1995). Although those experiments provide important parameters such as half-saturation constants for Co^{2+} (K_{mCo2+}) that could be species specific (Sunda and Huntsman, 1995), they do not allow studying the bioavailability of organic (CoL) and inorganic (Co′) Co species naturally present in the ocean. Considering that DCo was found to be predominantly organically bound in this study, it is important to study the bioavailability of organic Co. However, only one study has evidenced utilization of CoL by the cyanobacterium *Prochorococcus* (Saito et al., 2002).

In the present study, the biological uptake of Co by cyanobacteria, in addition to uptake by the most abundant phytoplankton nanoflagellates and dinoflagellates (Bown et al., 2011; Beker et al., 2012) may have significantly accounted for the strong DCo depletion observed in surface waters of the southern subtropical domain and northern subantarctic zone. In those waters, there was evidence of biological removal of CoL at the depths of DCo uptake (see above) further suggesting that Co could have been taken up by cyanobacteria, nano- and dinoflagellates, from the organic complexes. For instance, the growth rates of the coastal cyanobacterium *Synechococcus bacillaris* or *Prochlorococcus* are severely Co-limited at Co^{2+} concentrations below 3×10^{-14} M and 1×10^{-13} M respectively (Saito et al., 2002; Sunda and Huntsman, 1995). Thus the extremely low inorganic Co concentrations recorded in these waters (e.g. $[Co'] = 2 \times 10^{-20}$–$2 \times 10^{-18}$ M; Table 1) would have limited cyanobacteria growth very severely if the cells were unable to take up Co from CoL complexes. There is no K_m value for Co-limited growth of nanoflagellates and dinoflagellates available in the literature to evaluate any Co-limitation or non-limitation hypothesis in these waters. In any event, cyanobacteria (which have a known capacity to produce L) and nano- and dinoflagellates may be able to assimilate, directly or indirectly, CoL in the euphotic layer of the subtropical and north subantarctic domains.

Mechanisms of uptake of CoL are not known but the strong complexes, as exemplified by their high K'_{CoL} values, observed in this study, associated with their relative slowness for exchanging Co, suggest that they do not readily dissociate for inorganic Co uptake. The organic CoL complexes may not be available to some eukaryotic phytoplankton as previously suggested (Saito et al., 2004, 2005). On the other hand organic

Co can be directly bioavailable to some phytoplankton species, especially those with specialized uptake systems such as cobalophore and siderophore-like compounds (Duckworth et al., 2009), similar to the acquisition of iron with siderophores (Maldonado and Price, 2001; Shaked et al., 2005). In such a pathway, organic complexation of Co would thus enhance its availability to species able to take up organic CoL complexes, and may also increase the residence time of this pool, for example by slowing down rates of Co(II) oxidation to less soluble inorganic Co(III) species (Moffett and Ho, 1996) in the biologically oxygenated surface waters.

In surface waters of the ACC domain and the Weddell Gyre the relatively uniform distributions of DCo (Fig. 2; Bown et al., 2011) and CoL (Table 1) suggested a balance between the removal of Co and its sources. The Polar Front region was characterized by a spatially extensive post-diatom-bloom condition (Le Moigne et al., 2012). Diatoms dominated the phytoplankton biomass (Beker, 2012), and in the Weddell Gyre this assemblage contained degraded frustules with small or absent chloroplasts also suggesting a late stage of a relatively minor diatom bloom (Le Moigne et al., 2012). Nevertheless it has been suggested that biological uptake, especially by diatoms, may not have been the dominant mechanism for removal of DCo from these surface waters (Bown et al., 2011), probably because diatoms need much more iron and (to a lesser extent) zinc, than Co to grow (Sunda and Huntsman, 1995). Furthermore the higher DCo concentrations in those surface waters compared to those of the north of the section combined with the overall higher proportion of inorganic Co lead to inorganic Co concentrations as high as 11 pM in the post-diatom-bloom waters (Table 1). The inorganic Co concentrations (Co′) recorded in these waters were thus higher than the half-saturation Co^{2+} constant (K_{mCo2+}) reported for a coastal diatom *Thalassiosira pseudonana* ($K_{mCo2+} = 3.6\,10^{-12}$ M; Sunda and Huntsman, 1995), which presumably has a higher metals demand than its oceanic counterparts. In any event the oceanic diatom *Thalassiosira oceanica* is able to maintain relatively high growth rates (0.8–1.0 d^{-1}) even at low [Co^{2+}] ($\sim 10^{-14}$ M) without added zinc (Sunda and Huntsman, 1995); this further suggests that inorganic Co levels were not limiting the growth of the diatoms in the Polar Front region. Even *Phaeocystis Antarctica,* if present in those waters, would not have been limited by the inorganic Co concentrations (e.g. $K_{mCo2+} = 1.9\,10^{-13}$ M; Saito and Goepfert, 2008).

4.4 Potential impacts of the organic speciation on the geochemistry of cobalt

Benthic and sediment inputs, and transport from continental shelf and slope waters towards the open ocean, may be important sources of trace metals to the deep ocean (Bowie et al., 2002; Elderfield et al., 1981; Noble et al., 2008; Zhang et al., 2008b), notably for DCo (Noble et al., 2008; Huang and Conte, 2009; Bown et al., 2011). Processes by which DCo is released from sediments such as reductive processes in the sediments or dissolution of resuspended lithogenic particles in the overlying waters, as well as those by which it is advected to intermediate and deep ocean waters, are almost unknown. Previous sediment work has shown that cobalt could be recycled during dissolution and reprecipitation of sedimentary manganese oxides between suboxic and oxic sediments and pore waters (Heggie and Lewis, 1984). Reduction of Co(III) oxides from margin sediments and transport of the more soluble Co(II) in low oxygenated deep waters that intersect the margin are conceivable (Bown et al., 2011), as it has been proposed for manganese (Johnson et al., 1996). Deep Co inputs might also be stabilized as Co organic complexes, where the ligands are probably enhancing Co dissolution from the sediment rocks (Hausrath et al., 2009), which in turn generates high DCo concentrations in deep waters (Saito and Moffett, 2002). The advection of DCo from the margins of South Africa has been found in intermediate (I-AAIW) and deep (SE-NADW) waters in the subtropical domain (Bown et al., 2011). In those waters most DCo was organically bound (at 85–≥99.9 %; Table 1), suggesting that Co is transported from the lithogenic sources mainly as organic complexes in the cores of I-AAIW and SE-NADW. In addition, these intermediate and deep water masses were generally characterized by higher [Co′] ($\sim 1.0 \times 10^{-18}$ to 9.0×10^{-12} M) than what was found in surface waters, suggesting that a small but at times significant fraction of DCo (up to 15 %) is also transported as inorganic complexes in these waters.

These water cores discussed above have been identified in the section by their salinity signatures (>34.3 for I-AAIW, and >34.8 for SE-NADW) and by a dissolved oxygen maximum at 2000–3200 m for SE-NADW (Fig. 2, Table 2). Yet stabilization of oxidized Co(III) by organic complexation in these rather oxygenated waters appears to be the main pathway by which Co is advected from South Africa margins. It is possible that reduced inorganic Co(II) species still account for a smaller, but not trivial, fraction of the transported Co. In those water masses, reduced Co(II) species may indeed dominate the inorganic speciation of Co, with approximately 46 % of inorganic Co as free Co^{2+} ion, 22 % as sulfide inorganic complexes and 22 % as chloride complexes (Cosovic et al., 1982). The main reservoir of DCo along the section was found in the low-oxygenated Upper Circumpolar Deep Waters (A-UCDW and DP-UCDW, Fig. 2), due to remineralization and lithogenic inputs from the Drake Passage and the southwestern Atlantic along the fast eastward flow of the ACC (Bown et al., 2011). Hence it is possible that the maximum of [DCo] observed in these low-oxygenated waters results from the reduction of Co(III) oxides from margin sediments and transport of the more soluble Co(II) at the intersect of those water masses with margins and continental slopes (Bown et al., 2011), in addition to the remineralisation of DCo as Co(II) species in those waters.

Organic complexes represented more than 75 % of DCo in these waters (Table 1), which suggests that Co is transported predominantly as organic complexes. Similar observations were made in the Atlantic Ocean (Saito and Moffett, 2002). The redox state of the Co bound to these organic ligands is not known, but the rather low oxygen content of these water masses (160–190 μmol kg^{-1}) suggests that the Co(II) redox state may dominate. Hence the complexation of the more soluble Co(II) with organic chelates would probably promote the stabilization of Co in these waters. In addition, inorganic Co often accounted for a significant fraction of DCo, up to 25% (Table 1). Stabilization of inorganic reduced Co(II) species released from sediments at the South America continental slope, the Drake Passage and the Antarctic Peninsula, and produced by remineralization of DCo along the eastward ACC flow, was probably enhanced by the low O_2 contents of these water masses. It may have been further enhanced by low temperatures, which could slow down the kinetics of oxidation of inorganic Co(II) species into more insoluble inorganic Co(III) species (Lee and Fisher, 1993; Moffett and Ho, 1996). Finally, bottom enrichment of DCo in the Antarctic Bottom Waters was also evident, with increasing [DCO] along the water-mass pathway (Bown et al., 2011)..This may result from sediment resuspension and/or mixing with North Atlantic Deep waters in the Cape Basin. Similar trends of northward-increasing concentrations were observed for the organic ligands (Fig. 3) and organic Co (Table 1), and Co was more than 90 % organically complexed in those waters. Hence, in addition to suggesting that bottom sediments may be a source of Co chelators, this indicates that DCo from bottom sediments could be stabilized and transported predominantly as organic complexes. The organic speciation may thus prevent Co from being further scavenged after it has been released from bottom sediments.

5 Conclusions

The distribution of the organic Co-binding ligands suggests a biological source, potentially driven by cyanobacteria, in the subtropical domain and the northern subantarctic zone. In contrast, a rather conservative behaviour was observed in the central and south Antarctic Circumpolar Current (ACC) and the Weddell Gyre, which may reflect a balance between production and removal of Co-binding ligands. Dissolved cobalt occurred predominantly as organic complexes along the section. The production of Co-binding ligands may have enhanced the bioavailability of DCo in the subtropical waters to phytoplankton species with specialized CoL acquisition pathways, although mechanisms of organic Co uptake still need to be addressed. Biological uptake of organic Co would explain the nutrient like distribution of DCo observed in these waters (Bown et al., 2011). In surface waters of the ACC and Weddell Gyre inorganic Co concentrations were not at limiting levels, even though inorganic species were present at much lower concentrations than organic Co. In intermediate and deep waters, remineralization and advection of water masses that have been in contact with continental margins were sources of DCo (Bown et al., 2011), as well as organic ligands. The processes by which Co is released from the sediments (both reductive and non-reductive) need further investigation, yet this study has shown that sedimentary Co inputs are predominantly as organic complexes. In the intermediate and deep waters the complexation of Co with organic ligands may have promoted the stabilization of Co in the dissolved fraction, thus increasing its residence time over large scale of water-mass circulation.

Reduction of Co(III) oxides from margin sediments and transport of the more soluble inorganic Co(II) in the low oxygenated Upper Circumpolar Deep Waters may also be significant. Hence relatively high DCo concentrations in intermediate and deep waters appear to reflect sedimentary inputs, especially in the low oxygenated deep waters that intersect continental margins where the signature of these inputs was marked by a relative higher proportion of inorganic Co. More studies of the organic speciation of Co would be required to understand the interactions of Co with the phytoplankton communities, as well as the use of Co as a potential tracer of lithogenic sources in the intermediate and deep ocean.

Supplementary material related to this article is available online at: http://www.biogeosciences-discuss.net/9/3381/2012/ bgd-9-3381-2012-supplement.pdf.

Acknowledgements. We are most grateful for the assistance and the wonderful work at sea provided by Captain P. Courtes, the officers and the crew members of the French research vessel *Marion Dufresne II* during the IPY MD166 BONUS-GOODHOPE cruise. The co-chiefs scientists, M. Boye and S. Speich, andtheir collaborators M. Arhan (LPO, Brest, FR) and F. Dehairs (VUB, Brussels, Belgium) are warmly acknowledged for their efforts. We are grateful to the colleagues of our GO-FLO sampling team (Fanny Chever, Bronwyn Wake, Eva Buciarrelli, Géraldine Sarthou, François Lacanand Amandine Radic). This investigation was financed by theBONUS-GOODHOPE project and cruise funded by the French LEFE National Program of INSU, the National Agency of French Research(ANR-07-BLAN-0146-01)and the Paul Emile VictorInstitut. It is acontribution to the International Polar Year and the international GEOTRACESprogrammes. The Region Bretagne is supporting the PhD fellowship of J. Bown.

The publication of this article is financed by CNRS-INSU.

References

Arhan, M., Mercier, H., and Park, Y. H.: On the deep water circulation of the eastern South Atlantic Ocean, Deep-Sea Res. Pt. I, 50, 889–916, 2003.

Beker, B., Boye, M., Ras, J., Gelay, A., and Claustre, H.: Distribution patterns of taxonomy and pigments during the austral summer in the southeastern Atlantic and the Southern Ocean south of South Africa, for the Bonus-GoodHope Special Issue in Biogeosciences, in preparation, 2012.

Belkin, I. M. and Gordon, A. L.: Southern Ocean fronts from the Greenwich meridian to Tasmania, J. Geophys. Res.-Oceans, 101, 3675–3696, 1996.

Bonnet, S., Webb, E. A., Panzeca, C., Karl, D. M., Capone, D. G., and Sanudo-Wilhelmy,

S. A.: Vitamin B_{12} excretion by cultures of the marine cyanobacteria *Crocosphaera* and *Synechococcus*, Limnol. Oceanogr., 55, 1959–1964, 2010.

Bowie, A. R., Whitworth, D. J., Achterberg, E. P., Mantoura, R. F. C., and Worsfold, P. J.: Biogeochemistry of Fe and other trace elements (Al, Co, Ni) in the upper Atlantic Ocean, Deep-Sea Res. Pt. I, 49, 605–636, 2002.

Bown, J., Boye, M., Baker, A., Duvieilbourg, E., Lacan, F., Le Moigne, F., Planchon, F., Speich, S., and Nelson, D. M.: The biogeochemical cycle of dissolved cobalt in the Atlantic and the Southern Ocean south off the coast of South Africa, Mar. Chem., 126, 193–206, 2011.

Cosovic, B., Degobbis, D., Bilinski, H., and Branica, M.: Inorganic cobalt species in seawater, Geochim. Cosmochim. Ac., 46, 151–158, 1982.

Duckworth, O. W., Bargar, J. R., Jarzecki, A. A., Oyerinde, O., Spiro, T. G., and Sposito, G.: The exceptionally stable cobalt(III)-desferrioxamine B complex, Mar. Chem., 113, 114–122, 2009.

Elderfield, H., McCaffrey, R. J., Luedtke, N., Bender, M., and Truesdale, V. W.: Chemical Diagenesis in Narragansett Bay Sediments, Am. J. Sci., 281, 1021–1055, 1981.

Ellwood, M. J. and van den Berg, C. M. G.: Determination of organic complexation of cobalt in seawater by cathodic stripping voltammetry, Mar. Chem., 75, 33–47, 2001.

Ellwood, M. J., van den Berg, C. M. G., Boye, M., Veldhuis, M., de Jong, J. T. M., de Baar, H. J. W., Croot, P. L., and Kattner, G.: Organic complexation of cobalt across the Antarctic Polar Front in the Southern Ocean, Mar. Freshwater Res., 56, 1069–1075, 2005.

Gladyshev, S., Arhan, M., Sokov, A., and Speich, S.: A hydrographic section from South Africa to the southern limit of the Antarctic Circumpolar Current at the Greenwich meridian, Deep-Sea Res. Pt. I, 55, 1284–1303, 2008.

Gordon, A. L., Weiss, R. F., Smethie, W. M., and Warner, M. J.: Thermocline and Intermediate Water Communication between the South-Atlantic and Indian Oceans, J. Geophysic. Res.-Oceans, 97, 7223–7240, 1992.

Hausrath, E. M., Neaman, A., and Brantley, S. L.: Elemental release rates from dissolving basalt and granite with and without organic ligands, Am. J. Sci., 309, 633–660, 2009.

Heggie, D. and Lewis, T.: Cobalt in pore waters of marine sediments, Nature, 311, 453–455, 1984.

Huang, S. and Conte, M. H.: Source/process apportionment of major and trace elements in sinking particles in the Sargasso sea, Geochim. Cosmochim. Ac., 73, 65–90, 2009.

Johnson, K. S., Coale, K. H., Berelson, W. M., and Gordon, R. M.: On the formation of the manganese maximum in the oxygen minimum, Geochim. Cosmochim. Ac., 60, 1291–1299, 1996.

Le Moigne, F. A. C., Boye, M., Masson, A., Corvaisier, R., Grossteffan, E. , Guéneugues, A. and Pondaven, P.: Description of the biogeochemical features of the subtropical southeastern Atlantic and the Southern Ocean south off South Africa during the austral summer of the International Polar Year, for the BONUS-Goodhope Special Issue in Biogeosciences, submitted, 2012.

Lee, B. G. and Fisher, N. S.: Microbially mediated cobalt oxidation in seawater revealed by radiotracer experiments, Limnol. Oceanogr., 38, 1593–1602, 1993.

Maldonado, M. T. and Price, N. M.: Reduction and transport of organically bound iron by *Thalassiosira oceanica* (Bacillariophyceae), J. Phycol., 37, 298–309, 2001.

Martell, A. E. and Smith, R. M.: Critical stability constants, Plenum Press, New York, 495 pp., 1977.

Menzel, D. W. and Spaeth, J. P.: Occurrence of vitamin B_{12} in the Sargasso Sea, Limnol. Oceanogr., 7, 151–154, 1962.

Minas, H. J. and Packard, T. T.: Productivity in upwelling areas deduced from hydrographic and chemical fields, Limnol. Oceanogr., 31, 1182–1206, 1986.

Moffett, J. W. and Ho, J.: Oxidation of cobalt and manganese in seawater via a common microbially catalyzed pathway, Geochim. Cosmochim. Ac., 60, 3415–3424, 1996.

Morel, F. M. M., Milligan, A. J., Saito, M. A., Heinrich, D. H., and Karl, K. T.: Marine Bioinorganic Chemistry: The Role of Trace Metals in the Oceanic Cycles of Major Nutrients, Treatise on Geochemistry, Pergamon, Oxford, 113–143, 2003.

Noble, A. E., Saito, M. A., Maiti, K., and Benitez-Nelson, C. R.: Cobalt, manganese, and iron near the Hawaiian Islands: A potential concentrating mechanism for cobalt within a cyclonic eddy and implications for the hybrid-type trace metals, Deep-Sea Res. Pt. II, 55, 1473–1490, 2008.

Orsi, A. H., Whitworth, T., and Nowlin, W. D.: On the Meridional Extent and Fronts of the Antarctic Circumpolar Current, Deep-Sea Res. Pt. I, 42, 641–673, 1995.

Partensky, F., Hess, W. R., and Vaulot, D.: *Prochlorococcus*, a marine photosynthetic prokaryote of global significance, Microbiol. Mol. Biol. R., 63, 106–127, 1999.

Piola, A. R. and Gordon, A. L.: Intermediate Waters in the Southwest South-Atlantic, Deep-Sea Res. Pt. I, 36, 1–16, 1989.

Reid, J. L.: On the Total Geostrophic Circulation of the South-Atlantic Ocean - Flow Patterns, Tracers, and Transports, Prog. Oceanogr., 23, 149–244, 1989.

Ruzic, I.: Theoretical aspects of the direct titration of natural waters and its information yield for trace-metal speciation, Anal. Chim. Acta, 140, 99–113, 1982.

Saito, M. A. and Moffett, J. W.: Complexation of cobalt by natural organic ligands in the Sargasso Sea as determined by a new high-sensitivity electrochemical cobalt speciation method suitable for open ocean work, Mar. Chem., 75, 49–68, 2001.

Saito, M. A., Moffett, J. W., Chisholm, S. W., and Waterbury, J. B.: Cobalt limitation and uptake in *Prochlorococcus*, Limnol. Oceanogr., 47, 1629–1636, 2002.

Saito, M. A., Moffett, J. W., and DiTullio, G. R.: Cobalt and nickel in the Peru upwelling region: A major flux of labile cobalt utilized as a micronutrient, Global Biogeochem. Cyc., 18, 14 pp, 2004.

Saito, M. A., Rocap, G., and Moffett, J. W.: Production of cobalt binding ligands in a *Synechococcus* feature at the Costa Rica upwelling dome, Limnol. Oceanogr., 50, 279–290, 2005.

Saito, M. A., Goepfert, T. J., Noble, A. E., Bertrand, E. M., Sedwick, P. N., and DiTullio, G. R.: A seasonal study of dissolved cobalt in the Ross Sea, Antarctica: micronutrient behavior, absence of scavenging, and relationships with Zn, Cd, and P, Biogeosciences, 7, 4059–4082, doi:10.5194/bg-7-4059-2010, 2010.

Shaked, Y., Kustka, A. B., and Morel, F. M. M.: A general kinetic model for iron acquisition by eukaryotic phytoplankton, Limnol. Oceanogr., 50, 872–882, 2005.

Sunda, W. G. and Huntsman, S. A.: Cobalt and zinc interreplacement in marine phytoplankton: Biological and geochemical implications, Limnol. Oceanogr., 40, 1404–1417, 1995.

Turner, D. R., Whitfield, M., and Dickson, A. G.L.:. The equilibrium speciation of dissolved components in freshwater and seawater at 25 degrees C and 1 atm pressure, Geochim. Cosmochim. Ac., 45, 855–881, 1981.

van den Berg, C. M. G.: Determination of copper complexation with natural organic-ligands in sea-water by equilibration with MnO_2. 1. Theory, Mar. Chem., 11, 307–322, 1982.

van den Berg, C. M. G. and Kramer, J. R.: Determination of complexing capacities of ligands in natural-waters and conditional stability-constants of the copper-complexes by means of manganese-dioxide, Anal. Chim. Acta, 106, 113–120, 1979.

Whitworth, T. and Nowlin, W. D.: Water Masses and Currents of the Southern-Ocean at the Greenwich Meridian, J. Geophysic. Res.-Oceans, 92, 6462–6476, 1987.

Xue, Y. and Traina, S.: Oxidation kinetics of Co(II)-EDTA in aqueous and semi-aqueous goethite suspensions, Environ. Sci. and Technol., 30, 1975–1981, 1996.

Yang, R. J. and Van den Berg, C. M. G.: Metal complexation by humic substances in seawater, Environ. Sci. Tech., 43, 7192–7197, 2009.

Zhang, H., Van den Berg, C. M. G., and Wollast, R.: The determination of interactions of cobalt (II) with organic compounds in seawater using cathodic stripping voltammetry, Mar. Chem., 28, 285–300, 1990.

Zhang, Y., Jiao, N. Z., and Hong, N.: Comparative study of picoplankton biomass and community structure in different provinces from subarctic to subtropical oceans, Deep-Sea Res. Pt. II, 55, 1605–1614, 2008a.

Zhang, Y., Lacan, F., and Jeandel, C.: Dissolved rare earth elements tracing lithogenic inputs over the Kerguelen Plateau (Southern Ocean), Deep-Sea Res. Pt. II, 55, 638–652, 2008b.

Table 1. All data of the organic speciation of dissolved cobalt obtained in the southeastern Atlantic and the Southern Ocean during the MD166 BONUS-GoodHope cruise in 2008: dissolved cobalt concentrations (Bown et al., 2011; [DCo]), the organic cobalt-binding ligand concentrations ([L]), the conditional stability constant of Co-L complexes (K'_{CoL}), organic (CoL) and inorganic (Co′) cobalt concentrations and the percentage of organically bound dissolved cobalt.

Domain	Station	Latitude (° S)	Longitude (° E)	Depth (m)	DCo (pM)	Stdv DCo (pM)	L (pM)	Stdv L (pM)	log K'_{CoL}	CoL (pM)	(–)logCo′ (pM)	Organic cobalt (%)
STZ	L1	34.43	14.4	20	27.1	2.58	34.9	1.40	18.9	27.1	18.1	≥ 99.99
				40	29.7	2.55	35.1	0.80	18.8	29.7	17.8	≥ 99.99
				60	30.4	1.54	48.0	1.50	18.7	30.4	18.2	≥ 99.99
				80	29.9	0.67	32.7	1.90	18.5	29.9	17.2	≥ 99.99
				200	35.0	2.70	44.6	1.76	18.7	35.0	17.9	≥ 99.99
				700	50.1	3.09	39.3	1.00	19.3	39.3	11.0	78
				800	48.6	2.20	53.9	1.10	19.1	48.6	17.9	≥ 99.99
				1000	47.5	2.39	50.2	1.40	19.0	47.5	17.5	≥ 99.99
				1200	54.4	2.55	47.3	0.70	19.0	47.3	11.1	87
				2100	46.1	0.20	55.4	1.85	18.4	46.1	17.5	≥ 99.99
STZ	S1	36.5	13.1	20	23.7	2.15	47.8	0.67	16.6	23.7	16.4	≥ 99.99
				30	15.6	1.68	35.8	1.00	18.9	15.6	18.8	≥ 99.99
				40	26.3	1.97	34.9	1.00	19.2	26.3	15.5	≥ 99.99
				70	41.0	0.23	45.5	1.00	19.1	41.0	17.9	≥ 99.99
				100	44.3	0.73	45.2	2.00	19.2	44.3	17.2	≥ 99.99
				200	30.5	1.43	46.1	1.00	19.3	30.5	18.7	≥ 99.99
				300	37.6	2.80	44.3	2.00	19.1	37.6	18.1	≥ 99.99
				500	42.7	0.65	34.0	1.00	18.7	34.0	11.1	80
				700	51.8	0.53	52.5	1.00	19.1	51.8	16.9	≥ 99.99
				850	46.6	2.35	48.0	1.00	18.4	46.6	16.6	≥ 99.99
				1000	48.6	2.39	47.9	2.00	19.1	47.9	12.1	98
				1200	48.7	1.52	49.0	1.00	19.0	48.8	16.5	≥ 99.99
				1400	45.2	4.64	39.4	1.00	18.8	39.4	11.2	87
				1600	46.6	5.17	46.0	1.00	19.0	46.0	12.2	99
				2000	48.9	2.14	50.7	2.00	18.9	48.9	17.2	≥ 99.99
				2700	45.4	1.35	42.9	2.00	19.2	42.9	11.6	94
				3050	53.9	3.30	52.9	1.00	19.0	52.9	12.0	98
				3500	37.8	1.53	42.8	2.00	18.9	37.8	17.8	≥ 99.99
				3800	38.7	2.58	46.5	2.00	19.1	38.7	18.2	≥ 99.99
				4000	41.3	2.39	45.4	1.00	19.1	45.4	11.5	93
STZ	L2	41.18	9.92	15	17.0	0.54	71.9	2.80	18.5	17.0	18.8	≥ 99.99
				35	15.3	3.19	35.0	1.13	18.8	15.3	18.7	≥ 99.99
				45	19.0	0.23	35.5	0.77	18.8	19.0	18.5	≥ 99.99
				95	17.7	1.08	26.4	0.99	19.0	17.7	18.5	≥ 99.99
				300	46.6	5.63	48.7	1.31	19.1	46.6	17.5	≥ 99.99
				600	54.6	4.30	62.6	2.10	18.8	54.6	17.7	≥ 99.99
				800	54.0	3.33	49.4	1.24	19.7	49.4	11.3	91
				1200	46.3	0.95	39.0	1.18	19.7	39.0	11.1	84
				1400	45.9	1.44	47.3	0.72	19.2	45.9	17.4	≥ 99.99
				2100	49.2	2.38	52.7	0.64	20.3	49.2	18.9	≥ 99.99

Table 1. Continued.

Domain	Station	Latitude (° S)	Longitude (° E)	Depth (m)	DCo (pM)	Stdv DCo (pM)	L (pM)	Stdv L (pM)	log K'_{CoL}	CoL (pM)	(−)logCo' (pM)	Organic cobalt (%)
SAZ	S2	42.47	8.93	15	7.40	0.67	49.0	3.85	18.5	7.40	19.0	≥ 99.99
				30	5.73	1.15	35.6	0.80	19.0	5.73	19.5	≥ 99.99
				35	7.50	1.39	34.4	3.10	18.4	7.50	18.8	≥ 99.99
				196	38.2	0.99	69.2	5.80	17.9	38.2	17.5	≥ 99.99
				314	44.2	1.14	49.5	3.92	18.3	44.2	17.1	≥ 99.99
				461	52.1	2.66	32.8	2.68	18.5	32.8	10.7	63
				809	49.7	2.21	40.5	2.74	18.6	40.5	11.0	82
				1029	41.0	1.30	37.1	2.74	18.8	37.1	11.4	91
				1250	59.6	6.54	49.2	1.96	18.8	49.2	11.0	83
				1441	65.6	0.86	69.7	2.10	19.0	65.6	17.6	≥ 99.99
				1764	43.4	1.84	46.0	5.79	18.2	43.4	16.8	≥ 99.99
				2156	45.1	1.79	50.4	1.50	18.5	45.1	17.3	≥ 99.99
				2548	59.2	2.05	52.1	2.50	18.8	52.1	11.1	88
				3245	41.8	4.14	53.0	3.22	18.7	41.8	17.9	≥ 99.99
				3636	40.1	1.65	49.9	2.32	19.3	40.1	18.5	≥ 99.99
SAZ	L3	44.88	6.88	30	22.8	1.34	37.7	0.90	18.8	22.8	18.4	≥ 99.99
				100	38.7	0.83	46.7	1.60	19.3	38.7	18.3	≥ 99.99
				150	50.7	1.53	62.3	0.90	19.4	50.8	18.5	≥ 99.99
				270	49.3	2.50	58.4	2.20	19.0	49.4	18.0	≥ 99.99
				400	54.9	9.41	66.4	1.30	18.9	55.0	17.9	≥ 99.99
				600	47.2	3.56	53.8	2.70	18.8	47.2	17.7	≥ 99.99
				1200	49.5	1.04	55.7	1.40	19.2	49.5	18.1	≥ 99.99
				1400	51.9	1.21	51.6	1.60	18.9	51.6	12.5	99
				2100	47.1	1.01	41.0	1.10	19.2	41.0	11.2	87
SAZ	L4	46.01	5.87	30	27.3	×	44.9	3.60	18.2	27.3	17.7	≥ 99.99
				60	29.1	1.66	28.5	1.30	18.7	28.5	12.2	98
				100	48.2	1.90	29.5	1.70	18.5	29.5	10.7	61
				150	40.5	1.86	46.4	2.60	18.6	40.5	17.5	≥ 99.99
				270	52.9	1.28	46.0	1.30	18.8	46.0	11.2	87
				400	49.2	2.01	44.0	1.40	18.9	44.0	11.3	89
				800	48.7	2.12	39.9	1.70	19.0	39.9	11.1	82
				1300	45.9	2.32	44.5	1.80	18.6	44.5	11.9	97
				1600	50.3	0.50	38.5	1.20	19.0	38.5	10.9	77
				2050	45.5	2.53	32.0	2.20	18.8	32.0	10.9	70

Table 1. Continued.

Domain	Station	Latitude (° S)	Longitude (° E)	Depth (m)	DCo (pM)	Stdv DCo (pM)	L (pM)	Stdv L (pM)	log K'_{CoL}	CoL (pM)	(−)logCo' (pM)	Organic cobalt (%)
PFZ	S3	47.55	4.37	30	33.6	0.85	37.3	0.60	18.8	33.6	17.60	≥ 99.99
				70	35.7	1.27	44.4	3.00	18.3	35.7	17.40	≥ 99.99
				100	42.9	1.80	37.2	2.20	18.8	37.2	11.20	87
				200	40.5	2.17	37.8	1.50	18.8	37.8	11.60	93
				300	63.1	3.50	64.8	1.60	18.7	63.1	16.90	≥ 99.99
				450	50.1	0.30	49.8	2.40	18.4	49.8	12.50	99
				1500	42.3	0.28	35.1	1.60	19.2	35.1	11.10	83
				2020	39.5	1.84	43.6	1.60	18.9	39.5	17.60	≥ 99.99
				2500	40.7	3.22	49.2	1.10	19.2	40.7	18.30	≥ 99.99
				3000	36.6	0.91	63.4	2.00	19.1	36.6	18.70	≥ 99.99
				3500	33.3	3.20	40.5	0.80	18.9	33.3	18.00	≥ 99.99
				3980	30.5	0.27	38.0	1.20	19.1	30.5	18.30	≥ 99.99
PFZ	L5	49.03	2.84	40	43.5	2.33	35.5	2.80	18.2	35.5	11.10	82
				80	43.8	2.93	41.0	1.70	18.7	41.0	11.50	94
				150	42.2	3.23	44.3	1.10	19.2	42.3	17.60	≥ 99.99
				170	50.2	1.56	43.8	1.30	18.6	43.8	11.20	87
				250	49.0	0.95	39.8	1.70	18.6	39.8	11.00	81
				350	53.9	2.25	48.3	2.10	18.7	48.3	11.30	90
				700	72.9	4.51	63.6	2.60	18.8	63.6	11.00	87
				1600	46.0	1.10	50.8	1.60	18.9	46.0	17.70	≥ 99.99
				2200	39.9	1.26	47.7	2.60	19.1	39.9	18.10	≥ 99.99
North PF	L6	50.38	1.33	30	39.0	1.54	42.8	2.20	18.9	39.0	17.70	≥ 99.99
				60	37.8	3.27	38.6	2.40	19.0	37.8	17.10	≥ 99.99
				100	51.0	1.52	46.2	1.40	18.8	46.2	11.30	91
				135	58.7	2.19	60.5	2.00	18.9	58.7	17.20	≥ 99.99
				180	52.0	1.72	52.0	1.20	19.1	52.0	13.40	≥ 99.99
				300	48.6	0.46	47.5	1.90	19.2	47.5	12.00	98
				600	48.0	1.97	47.1	1.80	18.9	47.1	12.00	98
				850	45.1	3.06	48.9	1.30	18.9	45.1	17.60	≥ 99.99
				1600	39.5	2.22	49.6	1.10	19.1	39.5	18.20	≥ 99.99
				2100	36.5	1.74	44.7	1.70	18.9	36.5	18.00	≥ 99.99

Table 1. Continued.

Domain	Station	Latitude (° S)	Longitude (° E)	Depth (m)	DCo (pM)	Stdv DCo (pM)	L (pM)	Stdv L (pM)	log K'$_{CoL}$	CoL (pM)	(−)logCo′ (pM)	Organic cobalt (%)
South PF	S4	51.85	0	30	40.3	0.87	43.6	4.30	18.1	40.3	16.80	≥ 99.99
				60	37.6	2.10	35.0	2.20	18.2	35.0	11.60	93
				130	48.8	1.09	44.8	4.50	18.4	44.8	11.40	92
				160	45.6	2.55	52.1	1.10	19.0	45.6	17.90	≥ 99.99
				180	50.4	2.04	45.0	2.40	18.6	45.0	11.30	89
				250	56.8	1.40	49.7	2.50	18.8	49.7	11.10	87
				300	55.2	2.27	61.6	2.80	19.0	55.2	17.80	≥ 99.99
				350	49.6	1.33	49.2	1.80	18.9	49.2	12.40	99
				400	50.4	6.14	56.8	1.20	18.9	50.4	17.70	≥ 99.99
				500	50.1	1.66	42.1	0.80	18.9	42.1	11.10	84
				700	47.1	2.98	35.4	1.90	18.7	35.4	10.9	75
				1117	36.5	3.40	26.3	1.90	18.8	26.3	11.0	72
				1950	62.9	8.04	59.0	2.40	18.8	59.0	11.40	94
				2490	28.6	0.95	55.7	6.60	18.3	28.6	18.10	≥ 99.99
Sbdy	L7	55.23	0.03	30	51.3	1.11	52.0	1.80	19.1	51.3	17.00	≥ 99.99
				100	47.7	2.54	54.0	2.40	18.8	47.7	17.70	≥ 99.99
				120	49.7	1.88	49.4	2.60	18.7	49.4	12.50	99
				200	56.2	4.46	58.7	1.30	19.0	56.2	17.40	≥ 99.99
				300	49.5	3.15	56.0	1.80	19.1	49.5	18.00	≥ 99.99
				650	43.9	3.79	51.2	2.20	18.7	43.9	17.70	≥ 99.99
				1000	46.5	2.79	64.9	1.20	19.1	46.5	18.40	≥ 99.99
				1500	33.1	1.89	48.5	1.00	18.9	33.1	18.40	≥ 99.99
				2100	44.7	0.59	63.1	1.30	18.6	44.7	18.00	≥ 99.99
Weddell Gyre	S5	57.55	0.03	30	36.7	0.49	42.7	1.41	18.7	30.7	17.70	≥ 99.99
				60	36.0	0.60	49.8	4.50	18.2	22.2	17.5	≥ 99.99
				120	32.1	1.86	38.5	1.41	18.8	25.7	17.80	≥ 99.99
				250	43.4	1.23	38.5	2.53	18.9	43.4	11.30	89
				350	36.4	2.22	40.8	1.33	18.8	32.0	17.70	≥ 99.99
				450	39.7	2.74	35.7	2.50	18.6	39.7	11.40	90
				550	34.4	4.52	34.4	1.90	18.3	34.4	13.90	≥ 99.99
				800	37.6	4.03	37.2	0.80	18.6	37.6	12.40	99
				1250	30.1	1.91	35.2	1.88	18.7	25.0	17.70	≥ 99.99
				1700	38.4	0.65	43.7	0.75	19.2	33.1	18.10	≥ 99.99
				2150	32.9	1.26	36.1	2.21	18.5	29.8	17.30	≥ 99.99
				2600	33.3	3.01	44.0	1.28	18.7	22.6	18.0	≥ 99.99
				3500	29.1	1.01	32.1	1.10	18.9	26.2	17.60	≥ 99.99
				3840	30.5	0.32	33.2	1.26	18.7	27.7	17.50	≥ 99.99

Title Page
Abstract | Introduction
Conclusions | References
Tables | Figures
|◀ | ▶|
◀ | ▶
Back | Close
Full Screen / Esc
Printer-friendly Version
Interactive Discussion

Table 2. water masses origins, characteristics and depth ranges along the BONUS-Goodhope section

Water-mass	Origin	Characteristic(s)	Depth range (m)
North of the Agulhas Ridge (stations L1 to S2)			
I-AAIW: Indian Antarctic Intermediate Water[1]	Indian Ocean	salinity ≥ 34.3	800–1200 (L1 and S1)
A-AAIW: Atlantic Antarctic Intermediate Water[2]	Subantarctic region of the southwest Atlantic	salinity ≤ 34.3; $O_2 > 250\,\mu mol\,kg^{-1}$	600–1000 (L2 and S2)
A-UCDW: Atlantic Upper Circumpolar Deep Water[3]	Southwest Atlantic	oxygen minimum ($160–180\,\mu mol\,kg^{-1}$)	1200–1500 (L2 and S2)
SE-NADW: North Atlantic Deep Water[4–5]	North Atlantic ”southeastern route”	salinity >34.8	2000–3200
AABW: Antarctic Bottom Waters[6]	Weddell Sea	high oxygen, low temperature, low salinity	Below 3200
South of the Agulhas Ridge (stations L3 to S5)			
A-AAIW: Atlantic Antarctic Intermediate Water[1]	Subantarctic region of the southwest Atlantic	salinity ≤ 34.3; $O_2 > 250\,\mu mol\,kg^{-1}$	300–600 (L3 to L5)
A-UCDW: Atlantic Upper Circumpolar Deep Water[2]	Southwest Atlantic	oxygen minimum ($160–180\,\mu mol\,kg^{-1}$)	1000–1500 (L3 to L5)
DP-UCDW: Drake Passage Upper Circumpolar Deep Water[3]	Southern Ocean	oxygen minimum ($160–180\,\mu mol\,kg^{-1}$)	250–700 (L6 to L7)
SW-NADW: North Atlantic Deep Water[4–5]	North Atlantic ”southwestern route”	oxygen maximum	1500–3000 (L3 to L5)
AABW: Antarctic Bottom Waters[6]	Weddell Sea	high oxygen, low temperature, low salinity	Below 3500 (S3) below 3000 (S5)

[1]Gordon et al., 1992; [2]Piola and Gordon, 1989; [3]Withworth and Nowlin, 1987; [4]Arhan et al., 2003; [5]Gladyshev et al., 2008; [6]Reid, 1989

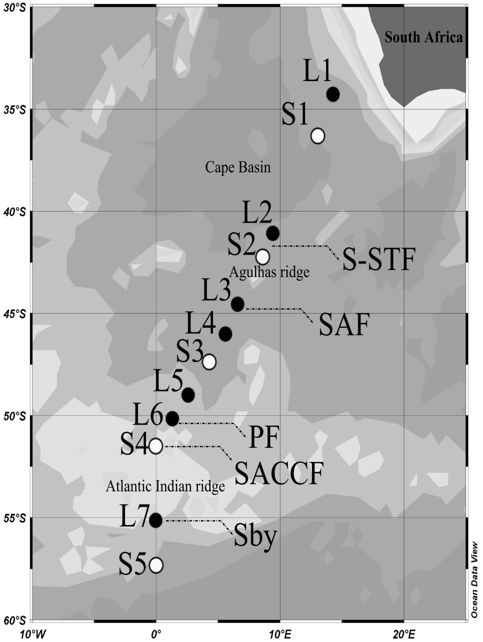

Fig. 1. Location of the stations sampled for DCo during the MD166 BONUS-GoodHope cruise. Black circles designate the LARGE stations and white circles the SUPER stations. The positions of fronts are also shown, with the southern branch of the Subtropical Front (S-STF; ∼42°2’S), the SubAntarctic Front (SAF; 44°2’S), the Polar Front (PF; 50°22.4’S), the Southern ACC Front (SACCF; ∼51°52’S) and the Southern Boundary of the Antarctic Circumpolar Current (SBdy; ∼55°54.3’S). From their geographical positions, stations L1, S1 and L2 were in the Subtropical Zone (STZ), S2 and L3 were, respectively, on the northern and southern side of the Subantarctic Zone (SAZ), stations L3, L4, S3 and L5 were within the Polar Frontal Zone, station L6 was on the northern flank of PF, S4 was on the SACCF, station L7 was at the Sby, and station S5 was in the northern branch of the Weddell Gyre. Map from ODV (Reiner Schlitzer).

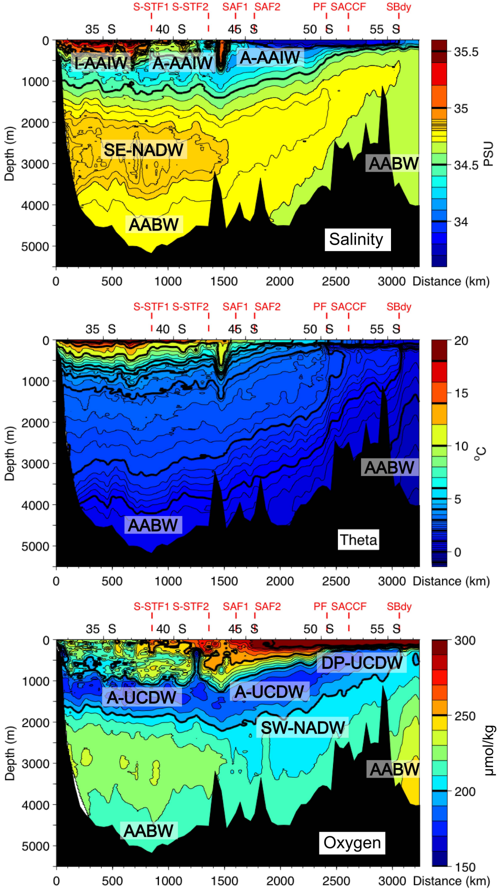

Fig. 2. Contour plots of salinity, potential temperature and oxygen versus depth (m) and latitude along the MD166 BONUS-Goodhope section (Speich et al., 2012).

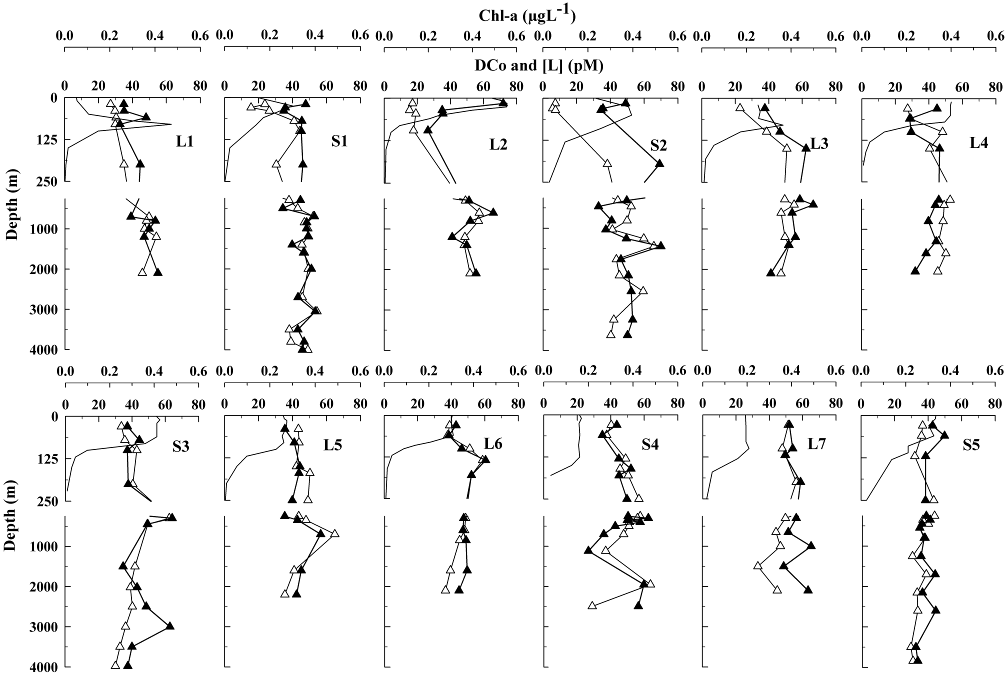

Fig. 3. Vertical distribution of the organic cobalt-binding ligands (L: black triangle and solid line, pM), dissolved cobalt (Bown et al., 2011; DCo: white triangle and solid line, pM), and Chlorophyll-*a* (Chl-*a*: solid line, μgL^{-1}) versus depth (m) at the LARGE and SUPER stations during the MD166 BONUS-GoodHope cruise. Chlorophyll-a data from (Guéneuguès and Boye, 2008).

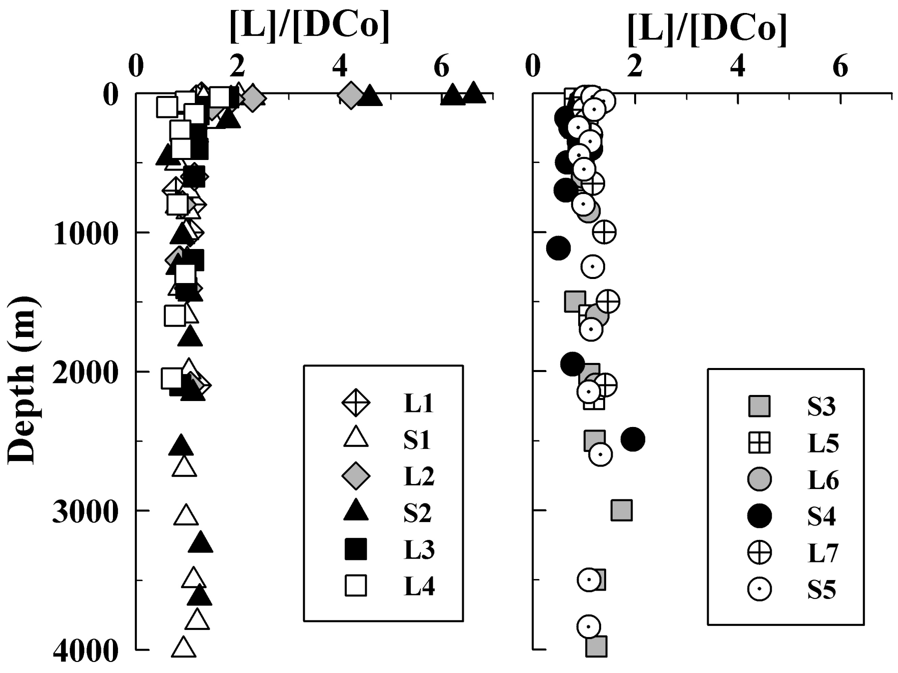

Fig. 4. Distribution at depth of L/DCo picomolar ratios. Note the different scales on L/DCo axis.

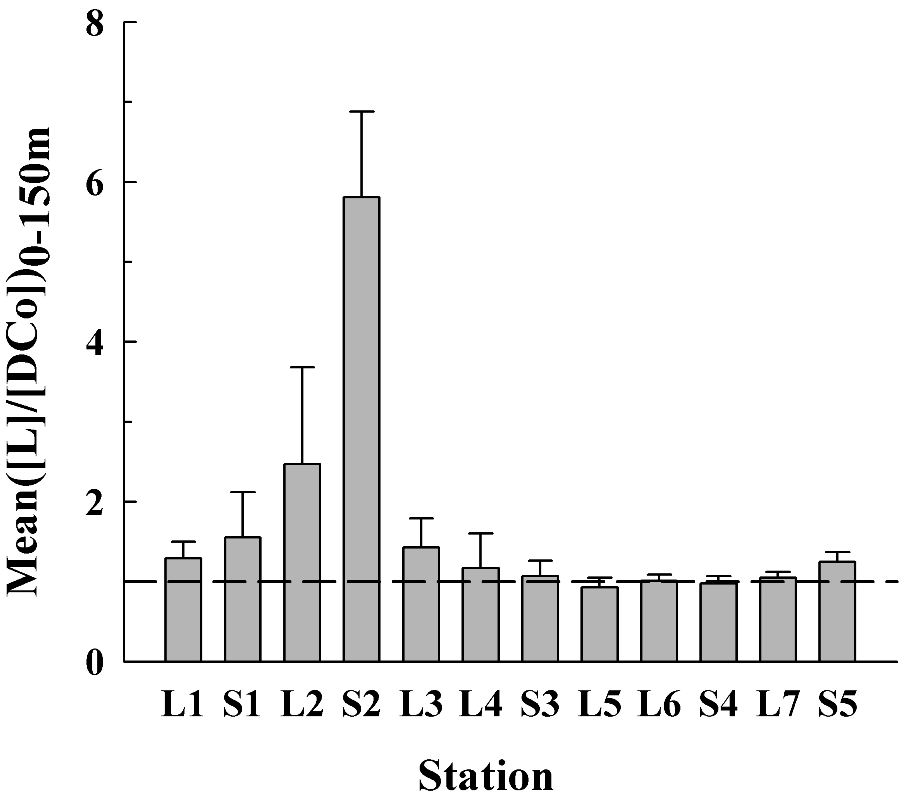

Fig. 5. Meridional trend of mean [L]/[DCo] picomolar ratios averaged in the upper 150 m at L and S stations (northern station is L1, southern is S5). Dashed line represent mean ([L]/[DCo]) = 1.

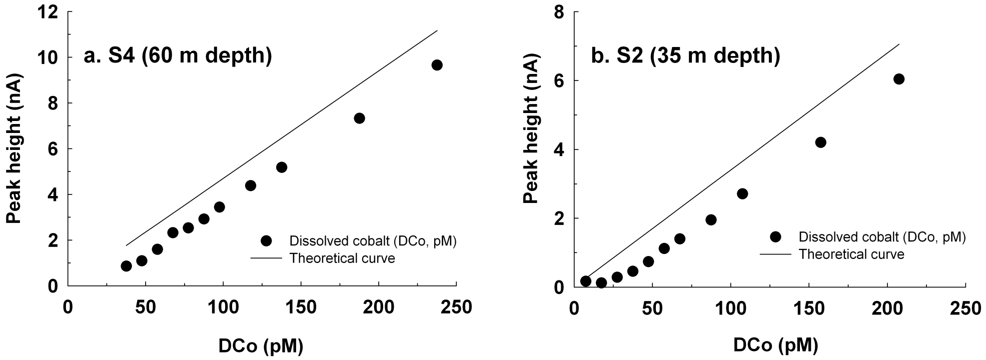

Fig. 6. Titration curves examples illustrating a lack of curvature (titration a) and the curvature (titration b).

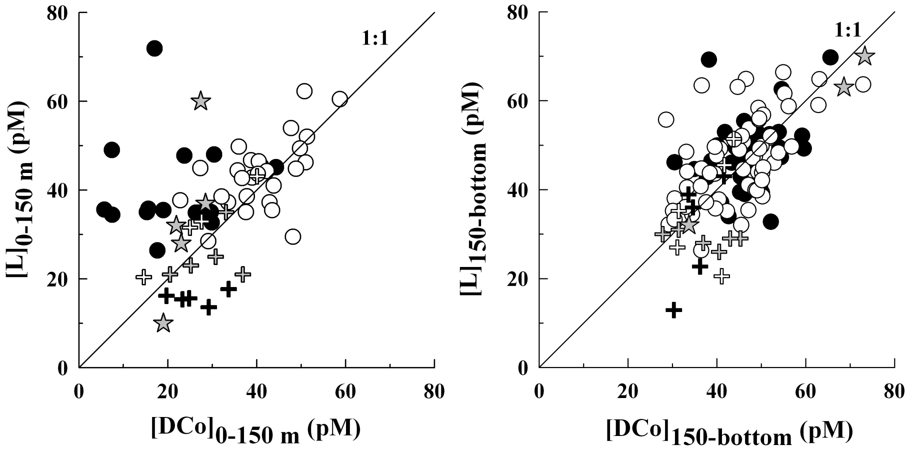

Fig. 7. Compilation of ocean data of organic Co-binding ligands (L, pM) versus dissolved cobalt (DCo, pM) concentrations in the top 150 m ocean waters (right panel) and in the deep waters below 150 m depth (left panel). Grey crosses = Ellwood and van den Berg, 2001; black (north of PF) and white (south of PF) crosses = Ellwood et al., 2005; grey stars = Saito et al., 2001; Black dots = this study, subtropical and northern subantarctic domains; White dots (this study, from L3 to S5 stations). The solid line represents the 1:1 line.